Geomatics, Natural Hazards and Risk
Vol. 1, No. 1, March 2010, 37–50

Taylor & Francis
Taylor & Francis Group

Appearance of extreme monsoonal rainfall events and their impact on erosion in the Himalaya

BODO BOOKHAGEN*
Geography Department, UC Santa Barbara, Santa Barbara, CA 93106-4060, USA

(*Received 10 January 2010; in final form 15 January 2010*)

Monsoonal rainfall in the Himalaya dominates erosion and sediment transport through the fluvial system. In addition to the strong seasonal nature of the Indian summer monsoon, striking interannual variations in monsoonal strength characterize longer records. For example, during any given year, rain may penetrate further into the orogen, even though peak rainfall amounts almost always occur at topographic barriers in regions with high relief, regardless of overall monsoonal strength. Tropical Rainfall Measurement Mission (TRMM) product 3B42 rainfall is first used to document the spatial rainfall distribution and then the TRMM time series are used to identify temporal and seasonal rainfall variations. A simple, but robust magnitude-frequency relation for each rainfall pixel is used to show that rainfall greater or equal to the 90th percentile occurs at least twice as often in mountainous terrain as in low-elevation regions. Previous field-based observations and measurements show that this significantly higher number of extreme events leads to higher erosion volumes and greater fluvial-mass transport rates. The spatiotemporal context of these extreme events helps to predict occurrences of high sediment flux and could underpin the strategic development of preventative measures. Improved statistics for extreme events are key to mitigating the filling of hydropower reservoirs and abrasion of hydropower turbines, as well as to sustaining infrastructure and successful agriculture in the downstream section of the Himalaya.

1. Introduction

Short-lived extreme weather events exert control on mass-transport processes and, hence, profoundly impact the character and rates of surface erosion processes (e.g. Baker and Kale 1998, Coppus and Imeson 2002, Hartshorn *et al*. 2002, Dadson *et al*. 2003, Snyder *et al*. 2003, Bookhagen *et al*. 2005a, Lague *et al*. 2005). In the Himalaya, interannual variations in the strength of the Indian summer monsoon strongly influence sediment flux and river discharge to the foreland (e.g. Sah and Mazari 1998, Paul *et al*. 2000, Barnard *et al*. 2001, Gabet *et al*. 2004, Bookhagen *et al*. 2005a, Singh *et al*. 2007). During large floods, as well as during abnormally wet monsoon years with elevated rainfall, large sediment volumes are transported through the fluvial system and transiently stored in the low-gradient reaches before ultimately reaching the oceans (e.g. Goodbred 2003). The rate of sediment transport

*Email: bodo@icess.ucsb.edu

Geomatics, Natural Hazards and Risk
ISSN 1947-5705 print/ISSN 1947-5713 online
http://www.tandf.co.uk/journals
DOI: 10.1080/19475701003625737

within the hydrologic cycle impacts both a diverse ecosystem and a population of more than 1 billion people (Ives and Messerli 1989, Stern 2007).

Flooding in the mountainous Himalaya and adjacent low-relief areas can be attributed mainly to two causes: (1) heavy or extreme rainfall events associated with synoptic climatic patterns; and (2) artificial and natural dam bursts. Both processes lead to a sudden increase of water overwhelming the fluvial system and increasing the fluvial transport capacity. Flood prediction related to extreme rainfall events is difficult because forecasting abilities of monsoonal rainfall are limited. Although the aberrant behaviour of the Indian monsoon is well documented, its characteristics and nature are not yet fully understood (e.g. Charles *et al*. 1997, Krishnamurthy and Shukla 2000, Gadgil *et al*. 2003, Kulkarni *et al*. 2009, Singh *et al*. 2009, Wulf *et al*. in press). Because both local factors and global teleconnections influence monsoon strength, a successful prediction of the Indian monsoon season is commonly deemed to be almost impossible (e.g. Webster 1987, Webster *et al*. 1998, Francis and Gadgil 2009, Rahman *et al*. 2009). In particular, rainfall observation and prediction in remote, high mountain terrains need to be improved. Coupled with extreme climatic events are mass-transport events, such as those triggered by excess rainfall amounts. A better assessment of the connection between these processes is desirable, but often difficult to achieve due to the lack of adequate monitoring possibilities.

The second flooding cause is catastrophic dam bursts often associated with glacial lake outburst floods (GLOFs) in the Himalaya (e.g. Richardson and Reynolds 2000, Kattelmann 2003, Meyer *et al*. 2006, Bajracharya *et al*. 2007). However, landslide lake outburst floods (LLOFs) are equally important and have a similar destructive nature (e.g. Shang *et al*. 2003, Dunning *et al*. 2006, Gupta and Sah 2008). In many cases, the formation of a lake and its rate of growth in remote, mountainous regions can be observed with repeated satellite imagery (e.g. Kääb and Vollmer 2000, Kääb 2002, Quincey *et al*. 2005, Bolch *et al*. 2008, Leprince *et al*. 2008, Scherler *et al*. 2008). If appropriate observations and warning mechanisms are in place, disasters can be avoided (e.g. Richardson and Reynolds 2000, Stern 2007, Korup and Clague 2009, Stone 2009). Today, post-flood identification is possible with multispectral satellite- or aerial-image analysis in the Himalaya. However, relating erosion processes with climatic triggering factors and developing a quantitative understanding of system response (the Earth's surface) to forcing magnitudes (rainfall amounts) requires different datasets and approaches.

In this study, rainfall data are utilized from the Tropical Rainfall Measurement Mission (TRMM) satellite, a joint mission between the US National Aeronautics and Space Administration (NASA) and the Japanese Aerospace Exploration Agency (JAXA). These data, recorded at 3-h intervals allow the identification of extreme events and their spatiotemporal context. Whereas these data cover only the last 11 years (1998–2008), several distinctive rainfall patterns help to delineate general relationships between rainfall, topographic relief and extreme-rainfall events. With this analysis, extreme events are not attempted to be predicted, but rather provide a framework for likely times and locations of extreme events.

This study falls in line with recently emerging discussions about varying magnitudes and discrepancies of climate change in the Himalaya (e.g. Cruz *et al*. 2007, Bhutiyani *et al*. 2008, Bagla 2009, Krishnamurthy *et al*. 2009, Raina 2009). The spatial asynchrony of climate change in the Himalaya is depicted by this regional analysis: climatic forcing throughout the Himalaya is not similar, as the Asian monsoon is a dynamic system tightly coupled to global teleconnections that change

their magnitudes at varying timescales (e.g. Webster 1987, Clemens *et al.* 1991, Clemens *et al.* 1996, Zhisheng *et al.* 2001, Anderson *et al.* 2002, Fleitmann *et al.* 2003, Gupta *et al.* 2003, Rahman *et al.* 2009). Thus, part of the difficulty in prediction is related to the different climatic-forcing time scales and time lags in system response to the observed processes. Previous publications have highlighted the impact of past, intensified monsoon phases that have significantly altered the Earth's surface by enhanced moisture transport into the orogen (e.g. Pratt *et al.* 2002, Clemens and Prell 2003, Staubwasser *et al.* 2003, Bookhagen *et al.* 2006, Clift *et al.* 2008, Owen *et al.* 2008, Dortch *et al.* 2009). For example, during the early Holocene an intensified monsoon period lasting roughly from 9 to 6 ka, moisture penetrated further into the orogen and entered regions that were previously and are arid today. This moisture increase most likely removed transiently stored sediments in the valley and led to the formation of large, deep-seated bedrock landslides that left a strong geomorphic imprint on the landscape (e.g. Gasse *et al.* 1991, Goodbred and Kuehl 2000, Bookhagen *et al.* 2005b, Dortch *et al.* 2009).

2. Methodology

2.1 *Tropical Rainfall Measurement Mission (TRMM) rainfall*

Tropical Rainfall Measurement Mission (TRMM) product 3B42 is used for analysis (Huffman *et al.* 2007). The data come in a gridded format with a spatial resolution of $0.25^\circ \times 0.25^\circ$ (~ 30 km $\times$ 30 km) and a temporal resolution of 3 h. Data access and detailed algorithm information are available on the web (http://disc.sci.gsfc.nasa.gov/precipitation/documentation/TRMM_README/TRMM_3B42_readme.shtml/). In short, input for the 3B42 dataset comes from two main sources: first, sensors onboard several low-earth-orbit satellites measuring indicators related to hydrometeors that ultimately result in surface precipitation. These sensors are the TRMM Microwave Imager (TMI), Special Sensor Microwave Imager (SSM/I), Advanced Microwave Scanning Radiometer-Earth Observing System (AMSR) and Advanced Microwave Sounding Unit-B (AMSU). Second, data from a geosynchronous satellite in the infrared spectrum are calibrated with the low-Earth-orbit satellites to provide high temporal observations of large parts of the Earth. In a final step, these datasets are combined through continuously improved and re-calibrated algorithms (Huffman *et al.* 2007).

Several studies suggest that the TRMM 3B42 surface-rainfall rate is comparable to the other surface observation (e.g. Koo *et al.* 2009, Sapiano and Arkin 2009), although the spatial scale of the rainfall data makes direct comparison to gauge data difficult. In addition, it has been argued that the TRMM 3B42 product is useful for creating a global landslide-hazard assessment (e.g. Hong *et al.* 2006).

2.2 *Spatiotemporal rainfall analysis*

The gridded dataset was used to create a rainfall climatology for the Himalaya and adjacent regions (figure 1). Mean annual and daily rainfall were calculated based on the 3-h measurement intervals over the time period from January 1998 to December 2008 (11 years). For all spatiotemporal analyses, daily rainfall amounts have been used as integrated from the 3-h data. Each gridded data cell or pixel in the landscape is treated separately to account for the local rainfall-intensity history. The

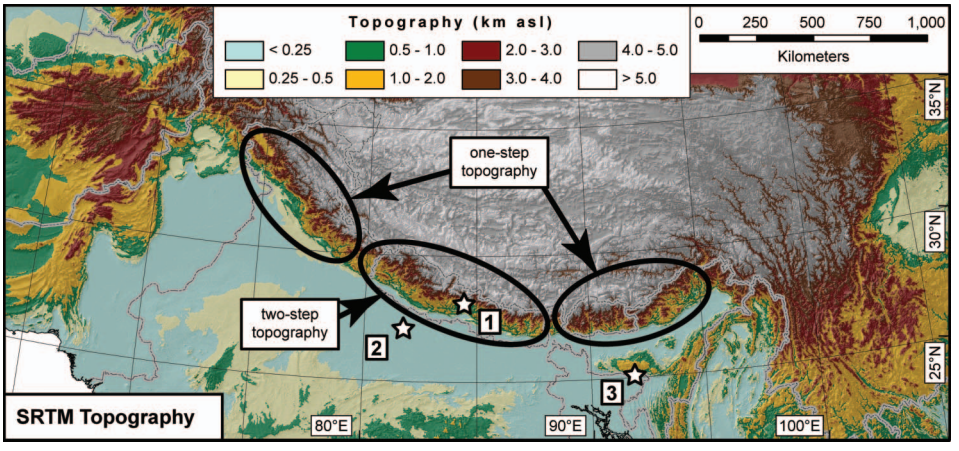

Figure 1. Topographic overview of the Himalayan and adjacent mountain ranges. International borders are outlined in grey. Western and eastern regions along the southern Himalayan front are characterized by a one-step topography. In contrast, the central Himalaya is characterized by a two-step topography that results in two distinctive rainfall peaks (cf. figure 7). White stars denote locations used in figure 2 to demonstrate extreme-rainfall determination using the 90th percentile as a lower limit.

probability density function was calculated for each pixel based on the 11-year measurement period to identify the 90th percentile (figure 2). That is, the rainfall time series was used to identify the occurrences (probabilities) of daily rainfall magnitudes. Rainfall in the 90th percentile has been previously associated with extreme rainfall events (e.g. Cayan *et al.* 1999, Grimm and Tedeschi 2009, Krishnamurthy *et al.* 2009). In other words, every rainfall event above the 90th percentile is defined as an extreme event. In a final step, the number of days per season that exceed the 90th percentile was counted. This count thus results in the number of extreme-rainfall days. For this study, the 90th-percentile rainfall based on the summer months (May–October) was calculated to demonstrate the importance of the Indian monsoon and to avoid the steep seasonal gradient.

3. Results

My analysis shows several important features: first, there exist two main rainfall gradients in the Himalayan realm (figure 3(*a*)): an approximately five-fold east-to-west gradient related to the distance from the moisture source (Bay of Bengal) and a ten-fold south-to-north rainfall gradient reaching from the monsoon-soaked Ganges Plain to the arid Tibetan Plateau that lies in the lee of the Himalayan orographic barrier. Second, mean daily summer (May–October) monsoon rainfall on the Ganges Plain ranges from 10 to more than 20 mm day^{-1} south of the Shillong Plateau (figure 3(*b*)). The Tibetan Plateau receives overall less than 5 mm day^{-1} rainfall, with significantly drier western areas. Third, summer (May–October) monsoon rainfall provides more than 80% of the annual moisture budget for large parts of the Ganges Plain and central Himalaya (figure 4). Far western and eastern areas receive lower rainfall amounts during the summer and thus their moisture budget is dominated by the westerlies, primarily during winter or by the East Asian monsoon. Fourth, my extreme rainfall analysis utilizing the 90th-percentile methodology shows that extreme rainfall amounts mimic to some degree the

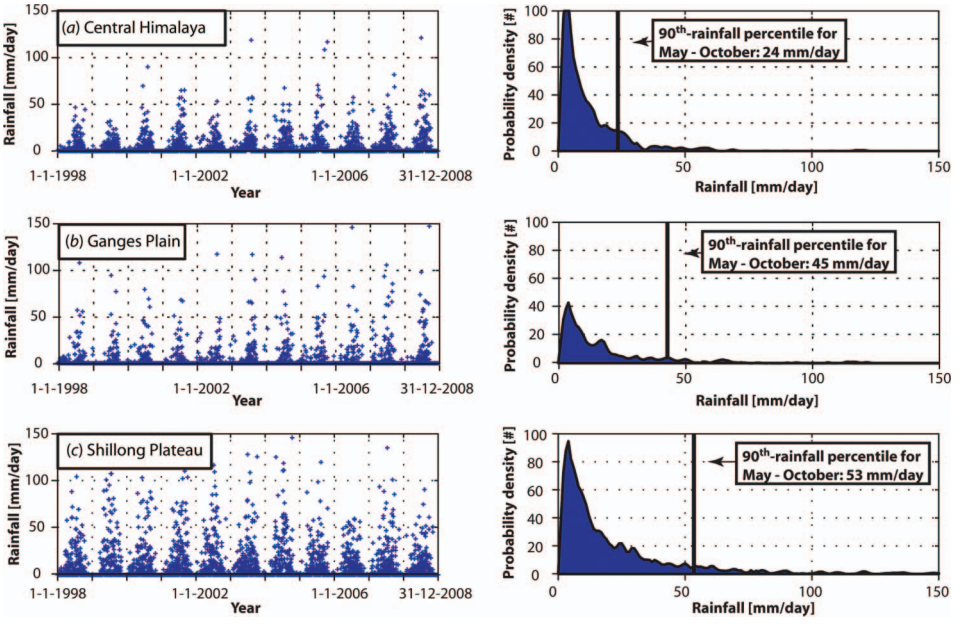

Figure 2. Example for calculating 90th-percentile rainfall. (*a*) Shows the TRMM 3B42 time series for a location in the central Himalaya (see figure 1 with label 1 for location). The right-hand panel shows probability density or number of occurrences in 1-mm day^{-1} bins as taken from the 11-year time series. The 90th-percentile for the summer season (May–October) at this location is 24 mm day^{-1}. (*b*) Displays a similar calculation for the Ganges Plain, which results in a 90th percentile of 45 mm day^{-1} during the summer season (see label 2 in figure 1). (*c*) Time series and probability density plot for the wettest inhabited place on Earth, the Shillong Plateau (see label 3 in figure 1). Note that the 90th percentile for the Shillong Plateau is more than twice as high as in the mountainous central Himalaya.

annual rainfall distribution (see for example figures 3(*a*) and 5). Note that the wettest inhabited place on Earth, south of the Shillong Plateau, receives more than 50 mm day^{-1} during an extreme rainfall event. Fifth, the number of extreme rainfall days varies widely through the study region, but remains relatively constant in mountainous terrain (figure 6). Despite the occurrence of higher extreme rainfall amounts in the low-elevation regions (figure 5), the occurrence of extreme events is nearly twice as high in mountainous terrain. In general, on the Ganges Plain there are less than 10 extreme rainfall days during one summer season, whereas there are more than 10 in the Himalaya. Mountain-peak areas are characterized by an even higher number of extreme rainfall events during one season. Note that this distribution is significantly decoupled from the overall rainfall pattern, as even areas with overall lower rainfall magnitudes have similar numbers of extreme-rainfall days.

4. Discussion

My rainfall data allow rainfall distribution in space and time to be deciphered. In this section, previously published findings and results from a high-spatial resolution, but low-temporal resolution rainfall dataset and field observations are summarized. Then, the high temporal but low spatial TRMM 3B42 data are used to identify temporal rainfall characteristics throughout the Himalaya.

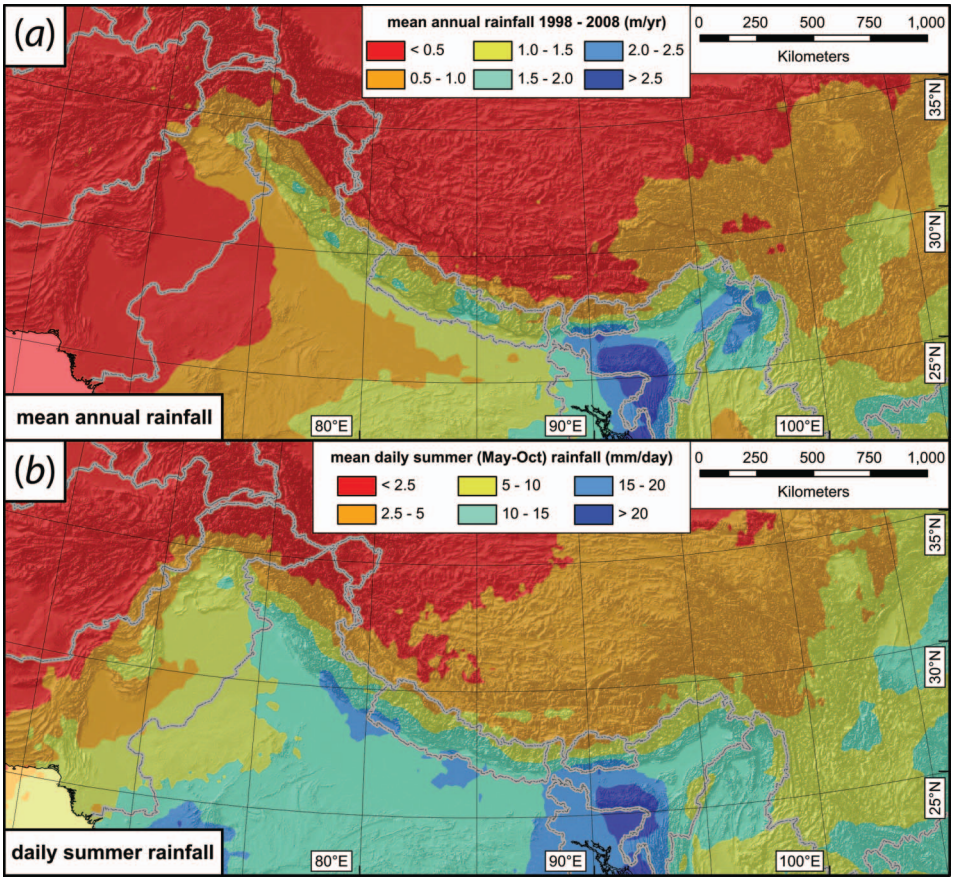

Figure 3. (*a*) Mean annual rainfall averaged over 11 years from 1998 to 2008 based on TRMM 3B42 data (see text). (*b*) Mean daily rainfall for the summer season (May– October) is derived from the same time series. The spatial resolution is 0.25° × 0.25° (~30 km × 30 km) and the temporal resolution is 3 h. Note the two dominant rainfall gradients in the Himalayan realm. First, an approximately five-fold east-to-west gradient reaching from the moisture source, the Bay of Bengal, to the Northwest Himalaya. Second, a ten-fold south-to-north gradient stretching from the monsoon-soaked Ganges Plains to the arid Tibetan Plateau that lies in the lee of the Himalayan orographic barrier.

4.1 *Spatial rainfall distribution*

Previously, several authors and myself have used the high spatial resolution Tropical Rainfall Measurement Mission (TRMM) rainfall product to analyse the impact of topography and relief on rainfall distribution (Anders *et al*. 2006, Bookhagen and Burbank 2006, in review, Bookhagen and Strecker 2008, Nesbitt and Anders 2009). Bookhagen and Burbank (2006, in review) identified elongate, range-parallel zones of high rainfall, and they demonstrated that topographic relief within a 3-km radius is a robust indicator for the location of rainfall-peak occurrence. Topographic relief is the difference between the minimum and maximum elevation within a given radius (e.g. 3 km). The topography and relief relationship can be tested in the Himalaya, because distinct topographic patterns exist (figure 1): the western and eastern Himalaya are characterized by a 'one-step' topography with steadily rising elevation

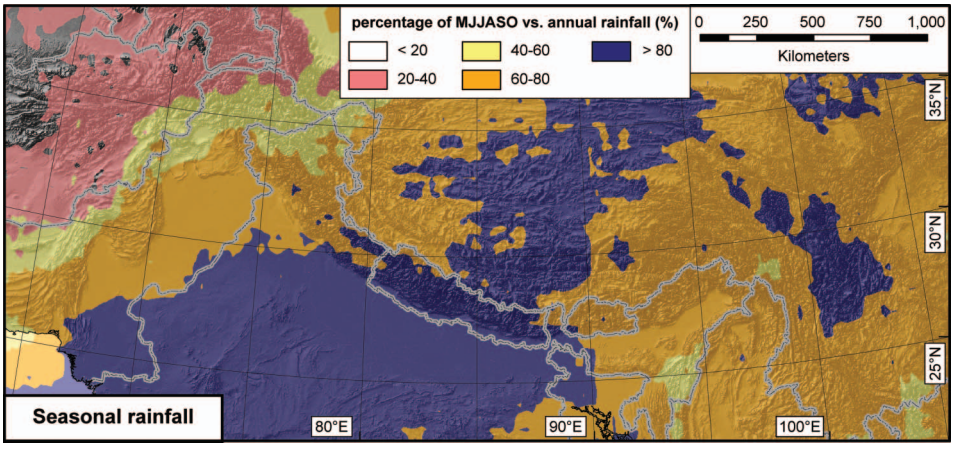

Figure 4. Summer monsoon rainfall as a percentage of annual rainfall amounts (from TRMM 3B42, see text). Blue areas indicate regions that receive more than 80% of their annual rainfall during the six summer months between May and October. Note that the far eastern and western areas of the Himalaya receive significant rainfall during the winter months as well.

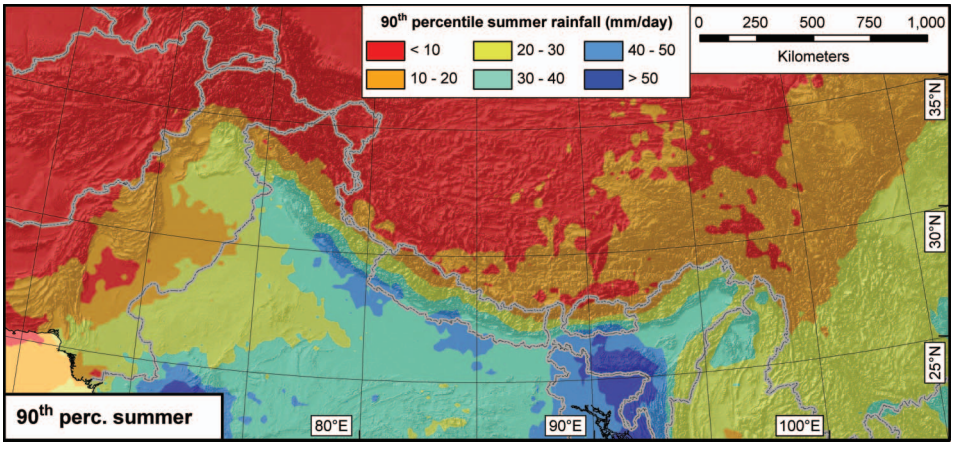

Figure 5. 90th-percentile summer (May–October) rainfall amounts as deduced from the 11-year TRMM 3B42 time series. The 90th percentile has been calculated only for the 6-month period to focus on the importance of the Indian summer monsoon and to avoid the steep seasonal rainfall gradient.

and a steep relief at the mountain front. In contrast, the central Himalaya is characterized by a 'two-step' topography, with a first topographic rise that displays moderate topographic relief associated with the geologic units of the Lesser Himalaya. The second, more dominant relief increase is associated with the geologic units of the Higher (or Greater) Himalaya, which also comprises the high Himalayan mountain peaks. In both regions, an abrupt increase in relief is associated with a rainfall peak.

Previous studies by Bookhagen and Burbank (2006, in review) show that the integrated moisture transport into the orogen is roughly similar along strike, despite a significantly different rainfall distribution (one versus two peaks) in the elevated

terrain. The topography-relief-rainfall relation is conceptualized in figure 7. Note that this synthesis does not allow prediction of a single storm (or rainfall event), but rather provides a general view of rainfall distribution averaged over several seasons. It is emphasized that the topography–rainfall relation can only be clearly delineated with the high spatial resolution TRMM data (e.g. TRMM product 2A12 or 2B31). In this study, we have used high temporal, but low spatial, resolution rainfall data to create an entire rainfall time series and capture all rainfall events.

In the Himalaya, intense rainfall events are often associated with high sediment fluxes (e.g. Paul *et al*. 2000, Barnard *et al*. 2001, Gabet *et al*. 2004, Bookhagen *et al*. 2005a, Wulf *et al*. in press). For example, in a previous study, Wulf *et al*. (in press)

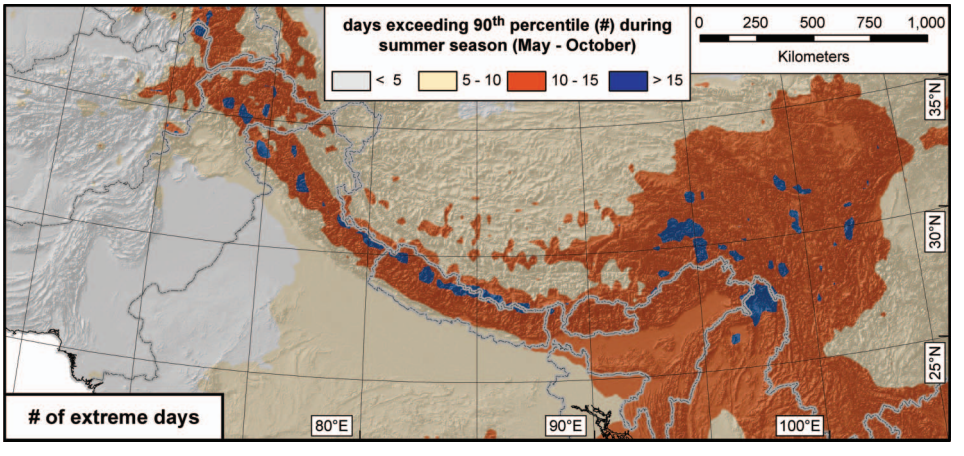

Figure 6. Spatial distribution of number of days within the 90th-percentile rainfall. See figure 3 for rainfall amounts associated with the 90th percentile. For each approximately 30 km × 30 km pixel, the 90th percentile has been calculated separately. Note that the mountainous Himalaya receive almost twice as many extreme rainfall days as compared to the surrounding regions.

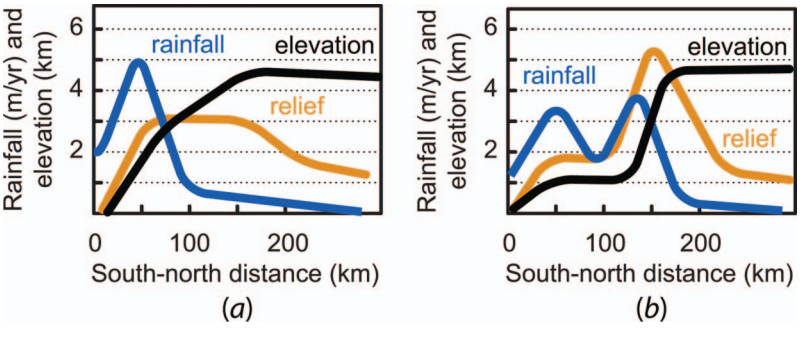

Figure 7. Simplified topography rainfall relation from the western and eastern Himalaya (*a*) and the central Himalaya (*b*) (see figure 1 for location details). Swaths are 50 km wide and 300 km long and were oriented perpendicular to the mountain front (Bookhagen and Burbank, in review). Shown here are averaged rainfall, elevation, and topographic relief within a 3-km radius along the profile for five profiles from each region. In general, rainfall-peak location correlates well with the steepest change of topographic relief (i.e. the slope of the relief distribution). Note that integrated rainfall amounts along a swath profile are roughly similar along strike.

showed that two extreme events lasting 5 days transported more than 50% of the entire suspended sediment budget during a 5-year period. Their study also showed that extreme rainfall events were associated with synoptic-scale climatic patterns that propagated from the mountain front into the usually dry orogen interior.

In a related study, Bookhagen *et al*. (2005a) showed that, during an abnormally strong monsoon year with extreme rainfall events, multiple debris flows and shallow landslides were triggered at a regional scale in a similar environment. Both study areas lie in the western Himalaya in the Baspa Valley, a transition zone between the wet, monsoon-soaked ranges to the south and arid regions to the north. In terms of the conceptualized topography-rainfall profile (figure 7), these regions lie on the descending, northern limb of the northern rainfall peak. Studies in the Marsyandi Valley in central Nepal provide similar results and suggest that the rainfall gradient during storm events that drive erosive discharge is about half as large as the gradient of seasonal rainfall (Gabet *et al*. 2004, 2008. Craddock *et al*. 2007).

This changing rainfall gradient during intense storms affects the region most sensitive to erosion during extreme rainfall events: climatic transition zones that lie just to the north of the rainfall peak. In these more arid, sparsely vegetated regions, intense rainfall has an amplified impact on mass-transport processes. The growing infrastructure and road construction in these areas will destabilize hillslopes even more and will lower the triggering threshold for debris flows and shallow landsliding. Moisture pathways into this region are provided by large valleys and low mountain passes (Bookhagen *et al*. 2005a). In these semi-arid to arid parts of the landscape, a large fraction of the total erosion appears to occur during these infrequent, but intense rainfall events (e.g. Paul *et al*. 2000, Barnard *et al*. 2001, Wulf *et al*. in press). This pattern is in stark contrast to the continuously, monsoon-soaked frontal or rainfall-peak regions, where rainfall of similar magnitude has a much lower erosional impact because dense vegetation and thick soil cover act as dampening components.

Similar conceptual relations were already suggested by Wolman and Miller (1960) in a semi-arid environment in the southwestern US. In order for the infrequent rainfall events to be an effective erosion agent, the landscape including soil and vegetation cover (often termed the 'critical zone') needs to be at its erosional threshold. In other words, several geomorphic processes resulted for the landscape to be in a sensitive state – voluminous erosional processes occur when a triggering threshold is exceeded, for example through intense rainfall events. The Himalaya and their steep rainfall gradient juxtapose a highly sensitive geomorphic threshold zone right next or immediately downwind of monsoon soaked regions. The high variability in monsoonal rainfall and its potential strengthening in the future increases the likelihood of erosive events from a region that is undergoing cultural development.

4.2 *Temporal rainfall distribution*

The seasonal rainfall map documents the spatial rainfall inhomogeneity during the summer season (figure 4). Large inhomogeneities exist in the spatiotemporal rainfall distribution in the Himalaya. The central Himalayan rainfall budget is dominated by the Indian monsoon during the summer. For example, the percentage of annual rain falling in the summer in Nepal and the central Ganges Plain is more than 80% (figure 4). This conclusion, based on remotely sensed data, supports earlier findings from rain-gauge stations located throughout India, but only sparsely distributed in

the mountains (Parthasarathy *et al*. 1992). Clearly, these regions require different hydrologic management than the neighbouring countries of India and Bhutan for which snowmelt plays a more significant role (e.g. Bookhagen and Burbank in review, Immerzeel *et al*. 2009).

My analysis shows for the first time that the eastern and western Himalaya receive only 60–80% of their annual moisture during the summer season. The far western Himalaya is more strongly influenced by the westerlies and receives less than 50% of its annual moisture during the Indian monsoon. These regions are furthermore characterized by high winter snowcover that results in snowmelt-runoff during the spring (e.g., Bookhagen and Burbank in review, Immerzeel *et al*. 2009).

Despite strong seasonal rainfall gradients, the entire Himalaya receives similar number of extreme rainfall days (figure 6). Even the generally drier NW Himalaya and Karakoram regions have similar numbers of extreme events. Despite expected data uncertainties, these along-strike similarities in event frequency are striking.

5. Conclusions

In this study, an analysis is provided of spatiotemporal rainfall distribution for the Himalaya and Tibetan Plateau. A gridded high temporal, low spatial Tropical Rainfall Measurement Mission (TRMM 3B42) dataset with 3-h sampling intervals at $0.25^\circ \times 0.25^\circ$ ($\sim$30 km $\times$ 30 km) spacing was utilized. These data reveal three key conclusions: first, in the central Himalaya and Ganges Plain more than 80% of the annual rainfall occurs during the Indian summer monsoon (May–October). Far western regions are influenced by the westerlies primarily. During the winter and summer, rainfall in these regions accounts for less than 50% of the total annual budget. Second, the spatial distribution of extreme rainfall events exceeding the 90th percentile is decoupled from the annual or seasonal rainfall distribution. In general, the mountainous Himalaya has almost twice as many extreme events as the Ganges Plain or the Tibetan Plateau, regardless of the rainfall amounts. Third, extreme events are more common in the dry interior rather than the wet exterior of the orogen. This important finding suggests the location of profound surface erosion to be in the lee of the orographic barrier where barren landscapes are susceptible to intense rainstorms.

Acknowledgments

The data used in this study were acquired as part of the Tropical Rainfall Measuring Mission (TRMM) sponsored by the Japan National Space Development Agency (NASDA) and the US National Aeronautics and Space Administration (NASA). This work was supported with grants from NASA (NNX08AG05G) and the National Science Foundation (EAR 0819874). I thank D. Burbank for discussions and comments.

References

Anders, A., Roe, G.H., Hallet, B., Montgomery, D.R., Finnegan, N.J. and Putkonen, J., 2006, Spatial patterns of precipitation and topography in the Himalaya. *GSA Bulletin Special Paper*, **398**, pp. 39–53.

Anderson, D.M., Overpeck, J.T. and Gupta, A.K., 2002, Increase in the Asian southwest monsoon during the past four centuries. *Science*, **297**, pp. 596–599.

Bagla, P., 2009, No sign yet of Himalayan meltdown, Indian report finds. *Science*, **326**, pp. 924–925.

Bajracharya, B., Shrestha, A.B. and Rajbhandari, L., 2007, Glacial lake outburst floods in the Sagarmatha region – hazard assessment using GIS and hydrodynamic modeling. *Mountain Research and Development*, **27**, pp. 336–344.

Baker, V.R. and Kale, V.S., 1998, The role of extreme floods in shaping bedrock channels. In *Rivers Over Rock: Fluvial processes in bedrock channels, Geophysics Monograph Series*, K.J. Tinkler and E.E. Wohl (Eds), pp. 153–165 (Washington, DC: AGU).

Barnard, P.L., Owen, L.A., Sharma, M.C. and Finkel, R.C., 2001, Natural and human-induced landsliding in the Garhwal Himalaya of northern India. *Geomorphology*, **40**(1–2), pp. 21–35.

Bhutiyani, M.R., Kale, V.S. and Pawar, N.J., 2008, Changing streamflow patterns in the rivers of northwestern Himalaya: implications of global warming in the 20th century. *Current Science*, **95**, pp. 618–626.

Bolch, T., Buchroithner, M.F., Peters, J., Baessler, M. and Bajracharya, S., 2008, Identification of glacier motion and potentially dangerous glacial lakes in the Mt. Everest region/Nepal using spaceborne imagery. *Natural Hazards and Earth System Sciences*, **8**, pp. 1329–1340.

Bookhagen, B. and Burbank, D.W., 2006, Topography, relief, and TRMM-derived rainfall variations along the Himalaya. *Geophysical Research Letters*, **33**, DOI: 2006GL026037.

Bookhagen, B. and Burbank, D.W., in review, Towards a complete Himalayan hydrologic budget: the spatiotemporal distribution of snow melt and rainfall and their impact on river discharge. *Journal of Geophysical Research-Earth Surface*, submitted.

Bookhagen, B. and Strecker, M.R., 2008, Orographic barriers, high-resolution TRMM rainfall, and relief variations along the eastern Andes, *Geophysical Research Letters*, **35**, DOI: 10.1029/2007GL032011.

Bookhagen, B., Thiede, R.C. and Strecker, M.R., 2005a, Abnormal monsoon years and their control on erosion and sediment flux in the high, and northwest Himalaya. *Earth and Planetary Science Letters*, **231**, pp. 131–146.

Bookhagen, B., Thiede, R.C. and Strecker, M.R., 2005b, Late Quaternary intensified monsoon phases control landscape evolution in the northwest Himalaya. *Geology*, **33**, pp. 149–152.

Bookhagen, B., Fleitmann, D., Nishiizumi, K., Strecker, M.R. and Thiede, R.C., 2006, Holocene monsoonal dynamics and fluvial terrace formation in the northwest Himalaya, India. *Geology*, **34**, pp. 601–604.

Cayan, D.R., Redmond, K.T. and Riddle, L.G., 1999, ENSO and hydrologic extremes in the western United States. *Journal of Climate*, **12**, pp. 2881–2893.

Charles, C.D., Hunter, D.E. and Fairbanks, R.G., 1997, Interaction between the ENSO and the Asian monsoon in a coral record of tropical climate. *Science*, **277**, pp. 925–928.

Clemens, S.C. and Prell, W.L., 2003, A 350,000 year summer-monsoon multi-proxy stack from the Owen ridge, Northern Arabian sea. *Marine Geology*, **201**, pp. 35–51.

Clemens, S., Prell, W., Murray, D., Shimmield, G. and Weedon, G., 1991, Forcing mechanisms of the Indian-Ocean monsoon. *Nature*, **353**, pp. 720–725.

Clemens, S.C., Murray, D.W. and Prell, W.L., 1996, Nonstationary phase of the plio-pleistocene Asian monsoon. *Science*, **274**, pp. 943–948.

Clift, P.D., Giosan, L., Biusztajn, J., Campbell, I.H., Allen, C., Pringle, M., Tabrez, A.R., Danish, M., Rabbani, M.M., Alizai, A., Carter, A. and Lueckge, A., 2008, Holocene erosion of the Lesser Himalaya triggered by intensified summer monsoon. *Geology*, **36**, pp. 79–82.

Coppus, R. and Imeson, A.C., 2002, Extreme events controlling erosion and sediment transport in a semi-arid sub-andean valley. *Earth Surface Processes and Landforms*, **27**, pp. 1365–1375.

Craddock, W.H., Burbank, D.W., Bookhagen, B. and Gabet, E.J., 2007, Bedrock channel geometry along an orographic rainfall gradient in the upper Marsyandi River valley in central Nepal. *Journal of Geophysical Research-Earth Surface*, **112**, DOI: 10.1029/2006JF000589.

Cruz, R.V., Harasawa, H., Lal, M., Wu, S., Anokhin, Y., Punsalmaa, B., Honda, Y., Jafara, M., Li, C. and Huu Ninh, N., 2007, *Asia* (Cambridge: Cambridge University Press).

Dadson, S.J., Hovius, N., Chen, H.G., Dade, W.B., Hsieh, M.L., Willett, S.D., Hu, J.C., Horng, M.J., Chen, M.C., Stark, C.P., Lague, D. and Lin, J.C., 2003, Links between erosion, runoff variability and seismicity in the Taiwan orogen. *Nature*, **426**, ppp. 648–651.

Dortch, J.M., Owen, L.A., Haneberg, W.C., Caffee, M.W., Dietsch, C. and Kamp, U., 2009, Nature and timing of large landslides in the Himalaya and Transhimalaya of northern India. *Quaternary Science Reviews*, **28**, pp. 1037–1054.

Dunning, S.A., Rosser, N.J., Petley, D.N. and Massey, C.R., 2006, Formation and failure of the Tsatichhu landslide dam, Bhutan. *Landslides*, **3**, pp. 107–113.

Fleitmann, D., Burns, S.J., Mudelsee, M., Neff, U., Kramers, J., Mangini, A. and Matter, A., 2003, Holocene forcing of the Indian monsoon recorded in a stalagmite from Southern Oman. *Science*, **300**, pp. 1737–1739.

Francis, P.A. and Gadgil, S., 2009, The aberrant behaviour of the Indian monsoon in June 2009. *Current Science*, **97**, pp. 1291–1295.

Gabet, E.J., Burbank, D.W., Putkonen, J.K., Pratt-Sitaula, B.A. and Ojha, T., 2004, Rainfall thresholds for landsliding in the Himalayas of Nepal. *Geomorphology*, **63**, pp. 131–143.

Gabet, E.J., Burbank, D.W., Pratt-Sitaula, B., Putkonen, J. and Bookhagen, B., 2008, Modem erosion rates in the High Himalayas of Nepal. *Earth and Planetary Science Letters*, **267**, pp. 482–494.

Gadgil, S., Shrestha, A.B., Wake, C.P., Dibb, J.E. and Mayewski, P.A., 2003, The Indian monsoon and its variability. *Annual Review of Earth and Planetary Sciences*, **31**, pp. 429–467.

Gasse, F., Arnold, M., Fontes, J.C., Fort, M., Gibert, E., Huc, A., Li, B.Y., Li, Y.F., Lju, Q., Melieres, F., Vancampo, E., Wang, F.B. and Zhang, Q.S., 1991, A 13,000-year climate record from Western Tibet. *Nature*, **353**, pp. 742–745.

Goodbred, S.L., 2003, Response of the Ganges dispersal system to climate change: a source-to-sink view since the last interstade. *Sedimentary Geology*, **162**, pp. 83–104.

Goodbred, S.L., and Kuehl, S.A., 2000, Enormous Ganges-Brahmaputra sediment discharge during strengthened early Holocene monsoon. *Geology*, **28**, pp. 1083–1086.

Grimm, A.M. and Tedeschi, R.G., 2009, ENSO and extreme rainfall events in South America. *Journal of Climate*, **22**, pp. 1589–1609.

Gupta, A.K., Anderson, D.M. and Overpeck, J.T., 2003, Abrupt changes in the Asian southwest monsoon during the Holocene and their links to the North Atlantic Ocean. *Nature*, **421**, pp. 354–357.

Gupta, V., and Sah, M.P., 2008, Impact of the Trans-Himalayan Landslide Lake Outburst Flood (LLOF) in the Satluj catchment, Himachal Pradesh, India. *Natural Hazards*, **45**, pp. 379–390.

Hartshorn, K., Hovius, N., Dade, W.B. and Slingerland, R.L., 2002, Climate-driven bedrock incision in an active mountain belt. *Science*, **297**, pp. 2036–2038.

Hong, Y., Adler, R. and Huffman, G., 2006, Evaluation of the potential of NASA multi-satellite precipitation analysis in global landslide hazard assessment. *Geophysical Research Letters*, **33**, DOI: 10.1029/2006GLO28010.

Huffman, G. J., Adler, R.F., Bolvin, D.T., Gu, G.J., Nelkin, E.J., Bowman, K.P., Hong, Y., Stocker, E.F. and Wolff, D.B., 2007, The TRMM multisatellite precipitation analysis (TMPA): quasi-global, multiyear, combined-sensor precipitation estimates at fine scales. *Journal of Hydrometeorology*, **8**, pp. 38–55.

Immerzeel, W.W., Droogers, P., de Jong, S.M. and Bierkens, M.F.P., 2009, Large-scale monitoring of snow cover and runoff simulation in Himalayan river basins using remote sensing. *Remote Sensing of Environment*, **113**, pp. 40–49.

Ives, J.D. and Messerli, B., 1989, *The Himalayan Dilemma: Reconciling development and conservation* (Chichester: John Wiley and Sons).

Kaab, A., 2002, Monitoring high-mountain terrain deformation from repeated air- and spaceborne optical data: examples using digital aerial imagery and ASTER data. *ISPRS Journal of Photogrammetry and Remote Sensing*, **57**, pp. 39–52.

Kaab, A. and Vollmer, M., 2000, Surface geometry, thickness changes and flow fields on creeping mountain permafrost: automatic extraction by digital image analysis. *Permafrost and Periglacial Processes*, **11**, pp. 315–326.

Kattelmann, R., 2003, Glacial lake outburst floods in the Nepal Himalaya: a manageable hazard? *Natural Hazards*, **28**, pp. 145–154.

Koo, M.S., Hong, S.Y. and Kim, J., 2009, An evaluation of the Tropical Rainfall Measuring Mission (TRMM) Multi-Satellite Precipitation Analysis (TMPA) data over South Korea. *Asia-Pacific Journal of Atmospheric Sciences*, **45**, pp. 265–282.

Korup, O. and Clague, J.J., 2009, Natural hazards, extreme events, and mountain topography. *Quaternary Science Reviews*, **28**, pp. 977–990.

Krishnamurthy, C.K.B., Lall, U. and Kwon, H.H., 2009, Changing frequency and intensity of rainfall extremes over India from 1951 to 2003. *Journal of Climate*, **22**, pp. 4737–4746.

Krishnamurthy, V. and Shukla, J., 2000, Intraseasonal and interannual variability of rainfall over India. *Journal of Climate*, **13**, pp. 4366–4377.

Kulkarni, A., Sabade, S.S. and Kripalani, R.H., 2009, Spatial variability of intra-seasonal oscillations during extreme Indian monsoons. *International Journal of Climatology*, **29**, pp. 1945–1955.

Lague, D., Hovius, N. and Davy, P., 2005, Discharge, discharge variability, and the bedrock channel profile. *Journal of Geophysical Research-Earth Surface*, **110**, DOI: 10.1029/2004JF000259.

Leprince, S., Berthier, E., Ayoub, F., Delacourt, C. and Avouac, J.P., 2008, Monitoring Earth surface dynamics with optical imagery. *EOS, Transactions*, **89**, pp. 1–2.

Meyer, M.C., Wiesmayr, G., Brauner, M., Hausler, H. and Wangda, D., 2006, Active tectonics in Eastern Lunana (NW Bhutan): implications for the seismic and glacial hazard potential of the Bhutan Himalaya. *Tectonics*, **25**, DOI: 10.1029/2005TC001858.

Nesbitt, S.W. and Anders, A.M., 2009, Very high resolution precipitation climatologies from the Tropical Rainfall Measuring Mission precipitation radar. *Geophysical Research Letters*, **36**, DOI: 10.1029/2009GL038026.

Owen, L.A., Caffee, M.W., Finkel, R.C. and Seong, Y.B., 2008, Quaternary glaciation of the Himalayan-Tibetan orogen. *Journal of Quaternary Science*, **23**, pp. 513–531.

Parthasarathy, B., Kumar, K.R. and Kothawale, D.R., 1992, Indian-Summer Monsoon Rainfall Indexes – 1871–1990. *Meteorological Magazine*, **121**, pp. 174–186.

Paul, S.K., Bartarya, S.K., Rautela, P. and Mahajan, A.K., 2000, Catastrophic mass movement of 1998 monsoons at Malpa in Kali Valley, Kumaun Himalaya (India). *Geomorphology*, **35**, pp. 169–180.

Pratt, B., Burbank, D.W., Heimsath, A. and Ojha, T., 2002, Impulsive alluviation during early Holocene strengthened monsoons, central Nepal Himalaya. *Geology*, **30**, pp. 911–914.

Quincey, D., Lucas, R.M., Richardson, S.D., Glasser, N.F., Hambrey, M.J. and Reynolds, J.M., 2005, Optical remote sensing techniques in high-mountain environments: application to glacial hazards. *Progress in Physical Geography*, **29**, pp. 475–505.

Rahman, S.H., Sengupta, D. and Ravichandran, M., 2009, Variability of Indian summer monsoon rainfall in daily data from gauge and satellite. *Journal of Geophysical Research-Atmospheres*, **114**, DOI: 10.1029/2008JD011694.

Raina, V.K., 2009, Himalayan Glaciers – A State-of-Art Review of Glacial Studies, Glacial Retreat and Climate Change, edited by M.O.E. Forsts, p. 60, Government of India.

Richardson, S.D. and Reynolds, J.M., 2000, An overview of glacial hazards in the Himalayas. *Quaternary International*, **65**, pp. 31–47.

Sah, M.P. and Mazari, R.K., 1998, Anthropogenically accelerated mass movement, Kulu Valley, Himachal Pradesh, India. *Geomorphology*, **26**, pp. 123–138.

Sapiano, M.R.P. and Arkin, P.A., 2009, An intercomparison and validation of high-resolution satellite precipitation estimates with 3-hourly gauge data. *Journal of Hydrometeorology*, **10**, pp. 149–166.

Scherler, D., Leprince, S. and Strecker, M.R., 2008, Glacier-surface velocities in alpine terrain from optical satellite imagery – accuracy improvement and quality assessment. *Remote Sensing of Environment*, **112**, pp. 3806–3819.

Shang, Y.J., Yang, Z.F., Li, L.H., Liu, D., Liao, Q.L. and Wang, Y.C., 2003, A super-large landslide in Tibet in 2000: background, occurrence, disaster, and origin. *Geomorphology*, **54**, pp. 225–243.

Singh, J., Yadav, R.R. and Wilmking, M., 2009, A 694-year tree-ring based rainfall reconstruction from Himachal Pradesh, India. *Climate Dynamics*, **33**, pp. 1149–1158.

Singh, M., Singh, I.B. and Muller, G., 2007, Sediment characteristics and transportation dynamics of the Ganga River, *Geomorphology*, **86**, pp. 144–175.

Snyder, N.P., Whipple, K.X., Tucker, G.E. and Merritts, D.J., 2003, Importance of a stochastic distribution of floods and erosion thresholds in the bedrock river incision problem. *Journal of Geophysical Research-Solid Earth*, **108**(B2), art. no. 2117.

Staubwasser, M., Sirocko, F., Grootes, P.M. and Segl, M., 2003, Climate change at the 4.2 ka BP termination of the Indus valley civilization and Holocene south Asian monsoon variability. *Geophysical Research Letters*, **30**, DOI: 10.1029/2002GL016822.

Stern, N., 2007, *Stern Review on the Economics of Climate Change* (Cambridge: Cambrdige University Press).

Stone, R., 2009, Perils in the Pamirs. *Science*, **326**, pp. 1614–1617.

Webster, P.J., 1987, *The Elementary Monsoon* (New York: John Wiley and Sons).

Webster, P.J., Magana, V.O., Palmer, T.N., Shukla, J., Tomas, R.A., Yanai, M. and Yasunari, T., 1998, Monsoons: processes, predictability, and the prospects for prediction. *Journal of Geophysical Research-Oceans*, **103**, pp. 14451–14510.

Wolman, M.G. and Miller, J.P., 1960, Magnitude and frequency of forces in geomorphic processes. *Journal of Geology*, **68**, pp. 54–74.

Wulf, H., Bookhagen, B. and Scherler, D., in press, Seasonal precipitation gradients and their impact on fluvial sediment flux in the Northwest Himalaya. *Geomorphology*, DOI: 10.1016/j.geomorph.2009.12.003.

Zhisheng, A., Kutzbach, J.E., Prell, W.L. and Porter, S.C., 2001, Evolution of Asian monsoons and phased uplift of the Himalayan Tibetan plateau since Late Miocene times. *Nature*, **411**, pp. 62–66.